Approved for Public Release; Distribution Unlimited
Case # 12-4898

Turbulence in Buoyant Jets using an Integral Flux Formulation

Jonathan T. Schwalbe, David B. Gouldey, and Joseph A. Hopper
The MITRE Corporation, McLean, VA 22102, USA
(Dated: December 10, 2012)

The turbulent kinetic energy (κ), and eddy dissipation rate (ϵ) for an axisymmetric turbulent buoyant jet are numerically determined. An outline of the derivation of the governing equations for these quantities from the time-averaged Navier-Stokes Equations is given. The Boussinesq approximation is adopted. An integral model is used to reduce the system of partial differential equations to one of ordinary differential equations by assuming Gaussian cross sections and quantities corresponding to the flux of κ and ϵ are found. This turbulence model is coupled with a well known model for the mean-field behavior of buoyant jets. Results from the integration of the system of equations are given as well as comparisons to experimental data for air/air jets which show agreement with the predicated output of the model.

PACS numbers:

I. INTRODUCTION

The dynamics of the effluent air from the exhaust stack of a powerplant, manufacturing facility, or other structure can have an impact on the environment, municipal planning, as well as aviation [1]. In the latter half of the last century, up through today, much work has been done to model this behavior. An excellent summary can be found in [2]. While many techniques have been adopted to examine this phenomena, of primary interest to this report are the integral models that have been created to model the behavior of jets and plumes [3, 4]. Through the past couple decades, these integral models have become more complex and have evolved to deal with increasingly general environmental conditions [5, 6].

Integral models can be derived by assuming a cross-sectional profile for the average quantities. Typical profiles leveraged are either the Gaussian distribution [2], which fits well with observation or a top-hat profile [7], which in many cases is less complicated. These models typically only calculate mean fluxes and report turbulent quantities by using constitutive equations. The experiments of Papanicolaou and List [8] show that turbulent kinetic energy accounts for 16% of the momentum and Jirka [2] points out that turbulent momentum and scalar fluxes are typically about 10% of the mean fluxes.

Many studies do not directly evolve the turbulent quantities using their respective transport equations. The justification for this is that the turbulent quantities are proportional to the mean quantities so there is no need for a separate representation [2]. However, Wang [9] argues that the turbulent quantities may vary between different regions of the buoyant jet and with different environmental conditions. Wang accounts for the turbulent quantities by treating them as an empirically varying percentage of the mean quantities, whereas other studies have used a fixed percentage [10].

The purpose of this paper is to extend the integral method of Reference [2] by adding evolution equations for the turbulent kinetic energy (κ) and eddy dissipation rate (ϵ). These equations are coupled to those of the mean flow to provide accurate predictions of the turbulent kinetic energy and the eddy dissipation rate in a variety of conditions. To the authors knowledge no integral model exists in the literature that evolves the turbulent kinetic energy separately or calculates the eddy dissipation rate using an integral flux formulation. In Section II, the problem statement will be given and relevant equations, coefficients, and boundary conditions will be developed. For the sake of brevity, many of the details are left to the cited literature (in particular the equations for the mean flow behavior), leaving the novel turbulence equations to this presentation. In Section III the results of the integration of the evolution equations will be compared to experimental data.

II. PROBLEM FORMULATION

Consider a cylindrical exhaust stack from a facility such as a power plant or manufacturing installation which has diameter D depicted in Figure 1. For the purposes of this study the height of the exhaust stack is of no relevance. For the remainder of this paper, this will be referred to as "the stack".

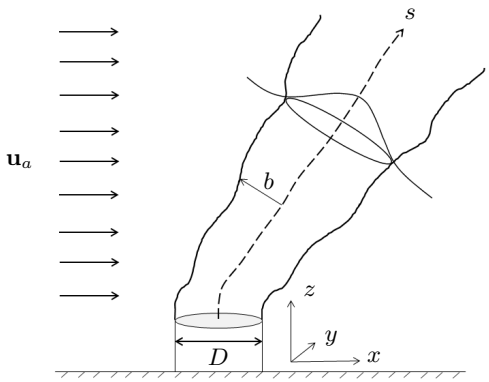

FIG. 1: A schematic of the problem.

The discharge from the stack is moving at a velocity U_0, and has a uniform density of ρ_0. An ambient uniform velocity field may be present ($\mathbf{u}_a$) which will orient the plume at an angle of $\theta(s)$ with respect to the x-axis where s is a coordinate representing the length of the centerline of the plume. The ambient conditions are given by density $\rho_a(z)$, pressure $p_a(z)$, and temperature $T_a(z)$. There exists a regions directly above the stack, known as the Zone Of Flow Establishment (ZOFE) described in [2], where the uniform efflux flow turns to fully developed jet flow. The top of the ZOFE is where boundary conditions are to be specified.

A. Governing equations

The flow of fluid out of the exhaust stack is governed by conservation of mass, momentum, and thermal energy, along with an equation of state relating density and temperature. In order to make this problem tractable, the convention is to separate the steady (U_i) and fluctuating (u_i) components of the velocity field. The Latin subscript i indicates spatial components of a vector; unless otherwise noted, summation is assumed for all repeated indices. For completeness, some of the relevant equations will be given here. Much of the derivation of the governing equations will be omitted from this presentation; the reader is referred to [11, 12] for complete details. The resulting time-averaged equations for conservation of mass, momentum, and thermal energy respectively are

$$\frac{\partial \rho U_i}{\partial x_i} = 0, \tag{1}$$

$$\rho \frac{D}{Dt}(U_i) = \frac{\partial}{\partial x_j}\left(\mu \frac{\partial U_i}{\partial x_j} - \rho \overline{u_i u_j}\right) - \frac{\partial p}{\partial x_i} + \rho g_i, \tag{2}$$

and

$$c_p \rho \frac{D}{Dt}(T) = \frac{\partial}{\partial x_i}\left(\lambda \frac{\partial T}{\partial x_i} - c_p \rho \overline{u_i T'}\right) \tag{3}$$

where D/Dt is the material derivative. In Eq. (2) μ is the molecular viscosity of the fluid. In Eq. (3) c_p is the specific heat at constant pressure and λ is the diffusivity of the medium. The term $\overline{u_i u_j}$ represents an unknown correlation between fluctuating velocities originating from the nonlinearity of the Navier-Stokes equations and the averaging process. This term is commonly known as the turbulent Reynolds' stress. The thermal energy equation also contains an unknown term representing the transport of heat due to turbulent processes, $\rho \overline{u_i T'}$. Here T' is the turbulent fluctuation in the temperature.

In order to close this system, governing equations for the quantities $\overline{u_i u_j}$ and $\overline{u_i T'}$ must be formulated.

1. *Equations for κ and ϵ*

The turbulent kinetic energy (κ), and eddy dissipation rate (ϵ) are defined as,

$$\kappa = \frac{1}{2}\overline{u_i u_i}, \tag{4}$$

and

$$\epsilon = -\nu \overline{\frac{\partial u_i}{\partial x_l}\frac{\partial u_i}{\partial x_l}}, \tag{5}$$

where ν is the molecular kinematic viscosity. After manipulation of the time-averaged and time-dependent governing equations [11, 13], the following evolution equations are found for κ and ϵ,

$$\frac{D}{Dt}(\kappa) = \frac{\partial}{\partial x_i}\left(c_s \frac{\kappa}{\epsilon}\overline{u_i u_l}\frac{\partial \kappa}{\partial x_l}\right) - P + G - \epsilon, \tag{6}$$

and

$$\frac{D}{Dt}(\epsilon) = \frac{\partial}{\partial x_i}\left(c_\epsilon \frac{\kappa}{\epsilon}\overline{u_i u_l}\frac{\partial \epsilon}{\partial x_l}\right) + c_{\epsilon 1}\frac{\epsilon}{\kappa}(P+G) - c_{\epsilon 2}\frac{\epsilon^2}{\kappa} \tag{7}$$

The terms P and G respectively represent the production of Reynolds' stress and the production or destruction of buoyancy and are given by

$$P = -\overline{u_i u_j}\frac{\partial U_i}{\partial x_j}, \tag{8}$$

$$G = -\beta g_i \overline{u_i T'}. \tag{9}$$

where $\beta = (1/\rho)(\partial \rho/\partial T)$ is the volumetric expansion coefficient where the derivative is taken at constant pressure. The reader should note that in writing Eq. (7) without a flux Richardson number, a vertical shear layer is assumed. In Eqs. (6) and (7) several empirical parameters are present which are determined from experiments. The values of these parameters are discussed in Appendix B. In addition to Eqs. (6) and (7), three algebraic expressions for $\overline{u_i u_j}$, $\overline{u_i T'}$, and $\overline{T'^2}$ can be found in [11] and are given in Appendix A.

B. Round Buoyant Jets

In this section, the equations governing the mean flow and turbulent dynamics will be specialized for the case when the buoyant jet is round and the initial flux is opposite the direction of gravity. The model developed here is valid beyond the ZOFE, where it is assumed that both the Reynolds ($Re = U_0 D/\nu$) and Grashof ($Gr = g(\rho_a - \rho_0)D^3/\rho_0 \nu^2$) numbers are sufficiently high so that the flow is entirely turbulent and all viscous effects can be neglected. Characteristic velocity and length scales have been chosen as U_0, and D, respectively. A cylindrical coordinate system is adopted where s is the vertical coordinate and r is the radial coordinate. U will denote the component of the velocity in the direction of

the main flow, and V in the radial direction. Buoyant jets contain regions depending on whether the flow is inertia or buoyancy dominated. The jet region is dominated by inertia while the plume region is dominated by buoyancy. With uniform velocity and density profiles at the efflux point, the Froude number is $Fr = U_0^2\rho_0/gD(\rho_a - \rho_0)$ and gives the relative importance of buoyancy and inertia. The characteristics of the environment into which the effluent air is released plays a role in determining the balance of inertia and buoyant forces.

Due to the nature of this shear layer flow the following boundary layer approximations is made,

$$V \ll U, \qquad \frac{\partial}{\partial s} \ll \frac{\partial}{\partial r} \tag{10}$$

Both static pressure and the pressure gradient in the mean flow direction are independent of the radial coordinate and hence $dp/ds = -\rho_a g$. Additionally, only steady processes are considered here and turbulent transport dominates over molecular transport. These assumptions greatly reduce the complexity of the governing equations for the mean flow and turbulent quantities.

1. Flux Formulation

At this point in the development, the system is composed of five partial differential equations and five auxiliary algebraic expression needed to close the system (the three in Appendix A broken into u and v components). These partial differential equations are converted to a set of ordinary differential equations by first assuming a Gaussian profile across each cross section of the flow,

$$\begin{aligned} U &= u_c e^{-r^2/b^2} + u_a\cos(\theta), \quad & T &= T_c e^{-r^2/(\sigma_T b^2)} \\ \kappa &= \kappa_c e^{-r^2/(\sigma_\kappa b^2)}, & \epsilon &= \epsilon_c e^{-r^2/(\sigma_\epsilon b^2)}, \end{aligned} \tag{11}$$

where the subscript c denotes the value on the centerline of the flow, and integrating each term across the flow,

$$\int_A (\cdot) dA \tag{12}$$

where A is the cross section area element and $dA = rdrd\theta$. The quantity $b(s)$ denotes the radial distance where the velocity has decreased by a factor of $e^{-1}u_c$, where u_c is the centerline velocity of the plume. Applying the assumptions from the previous section and integrating each term using Eq. 12 the following equations are found which govern the dynamics of the flux of κ, and ϵ

$$\begin{aligned} \frac{d}{ds}(\Sigma) =& C_\mu K_1 \frac{\kappa_c^2}{\epsilon_c} u_c^2 + K_2 \beta g \frac{\kappa_c^3}{\epsilon_c^2} u_c T_c - \\ & K_3 \beta^2 g^2 \frac{\kappa_c^4}{\epsilon_c^3} t_c^2 - \frac{1}{2} b^2 \epsilon_c, \end{aligned} \tag{13}$$

and

$$\begin{aligned} \frac{d}{ds}(\Phi) =& C_\mu c_{\epsilon 1} M_1 \kappa_c u_c^2 - M_2 c_{\epsilon 1} \frac{\kappa_c^2}{\epsilon_c} u_c - \\ & M_3 c_{\epsilon 1} \frac{\kappa_c^3}{\epsilon_c^2} - c_{\epsilon 2} M_4 b^2 \frac{\epsilon_c^2}{\kappa_c}. \end{aligned} \tag{14}$$

The quantities Σ and Φ represent the flux of κ and ϵ through a cross section of the flow. The point-wise quantities are computed using

$$\Sigma = b^2 \left(u_c \frac{\sigma_\kappa}{1+\sigma_\kappa} + u_a \sigma_\kappa \cos(\theta) \right) \kappa_c, \tag{15}$$

$$\Phi = b^2 \left(u_c \frac{\sigma_\epsilon}{1+\sigma_\epsilon} + u_a \sigma_\epsilon \cos(\theta) \right) \epsilon_c. \tag{16}$$

The expressions for the quantities C_μ, $\{K_i\}$, and $\{M_i\}$ can be found in Appendix B. The algebraic expressions from Appendix A have been incorporated in Eqs. (13) and (14). The equations governing the dynamics of the mass, momentum, and temperature flux from which the mean centerline velocity (u_c) and temperature (T_c) are derived can be found in [2] and are not reproduced here.

2. Initial Conditions

In general, initial conditions for a buoyant jet at a power plant or manufacturing facility are given at the top of the stack. This is the beginning of the ZOFE however the domain of the system in question here begins at the end of the ZOFE. Conditions for the mean flow quantities at the top of the ZOFE are given in [2]. What is needed therefore are conditions for the turbulent quantities once the fully turbulent flow is established. Following the discussion in [8], the quantities $\overline{u}/U = b_1$ and $\overline{v}/U = b_2$ are constant throughout the flow. This yields the following constant quantity

$$\kappa = \frac{1}{2}(b_1^2 + 2b_2^2)U^2 = C_\kappa U^2 \tag{17}$$

where $C_\kappa = 0.06$. The initial conditions for κ at the beginning of the turbulent flow is therefore $\kappa_0 = 0.06U_0^2$. According to the work of [14], the dimensionless quantity

$$C_\epsilon = 3b_{0.5}\epsilon/(2\kappa)^{3/2} \tag{18}$$

is constant throughout the flow where $b_{0.5}$ is the half-velocity radius. The quantities b and $b_{0.5}$ are related by the constant $b_3 = b/b_{0.5} \approx 1.2$. Leveraging Eq. 17 and rearranging the expression for C_ϵ yields

$$\epsilon = \frac{2^{3/2}}{3} C_\epsilon b_3 C_\kappa^{3/2} \left(\frac{U^3}{b} \right) = 0.018 \left(\frac{U^3}{b} \right). \tag{19}$$

The initial condition for ϵ at the beginning of the fully established turbulent flow is $\epsilon_0 = 0.018U_0^3/b_0$. It should be noted that the authors of [14] referenced multiple values of C_ϵ; this may change the initial value of ϵ to $\epsilon_0 = 0.019U_0^3/b_0$.

III. RESULTS

In this section, results from integration of the equations for the mean flow [2] coupled to Eqs. 13 and 14 using MATLAB's ODE45 routine and the initial conditions discussed in the previous section are obtained. The evolution of κ, and ϵ are shown with varying initial conditions. Experiments have been performed which measure the turbulent fluctuations of the mean velocity field (u_i') which can be used as a point of comparison for numerical solutions to the governing equations.

A. Dynamics of κ and ϵ

Parameters of interest are the diameter of the exhaust stack, the velocity of the effluent at the exit point of the stack, and the difference in temperature of the effluent and the ambient conditions. Calm ambient conditions will be assumed. Figure 2 shows the effect of varying the stack diameter on the evolution of κ and ϵ. Varying the stack diameter has a greater effect on ϵ than it does on κ. The variance scaled by the square of the mean of the distributions of κ and ϵ at a height of 100 diameters above the stack are 0.0049 and 1.11, respectively, indicating that the eddy dissipation rate of the system is more sensitive to changes in exit stack diameter than the turbulent kinetic energy. To further investigate the response of the system to changes in stack diameter, Figure 3 shows changes in κ and ϵ, scaled by their initial values at the top of the ZOFE, at a downstream distance of $100D$ as a function of stack diameter. With respect to the scaled variables, the anticipated tradeoff of decreasing κ with increasing ϵ is seen here.

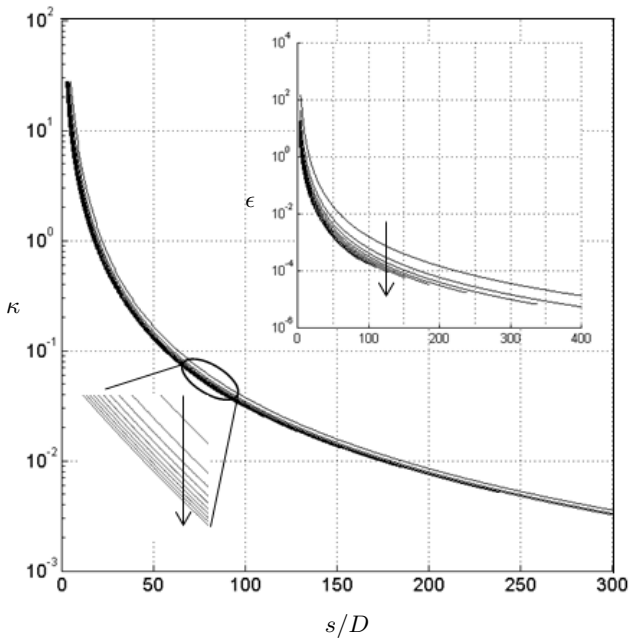

FIG. 2: Evolution of κ and ϵ (inset) with a varying stack diameter. The stack diameter was varied from 2m to 47m in steps of 5m. The arrows indicate the direction of increasing stack diameter. Relevant model parameters were $c_{\epsilon 1} = 1.44$, $c_{\epsilon 2} = 2.02$, $c_{1T} = 3.0$, $c_{2T} = 0.5$, $c_{3T} = 0.8$, $R = 0.8$, $\sigma_\kappa^{1/2} = 1.343$, $\sigma_\epsilon^{1/2} = 1.505$, and $\sigma_T^{1/2} = 1.20$.

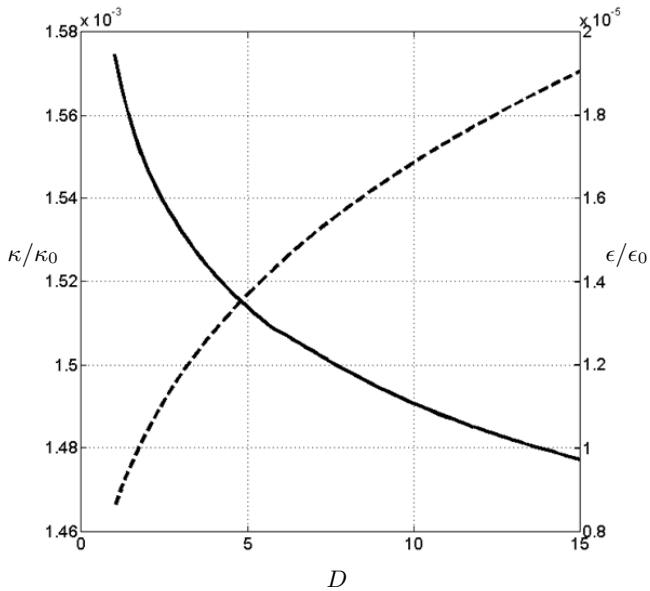

FIG. 3: Values of κ (solid) and ϵ (dashed) scaled by their initial values at an downstream distance of 100 stack diameters above the exit point for varying stack diameters. Relevant model parameters and initial values are the same as those in Figure 2.

Figure 4 illustrates the system's response to a varying effluent velocity at the stack exit point. It is seen that increasing the exit velocity increases the turbulent kinetic energy and eddy dissipation rate. Increasing excess effluent temperature causes an monotonic increase in κ at all elevations above the stack. This is not the case with ϵ. Figure 5 shows the change in κ and ϵ at two elevations above the exit point of the stack. At a particular (and sufficient) height above the stack, ϵ exhibits a local maximum as a function of excess temperature. Figure 6 gives the excess initial temperature where the local maximum occurs as a function of vertical location. For the values of the model parameters chosen for this study (see caption from Figure 2), the minimum location where a local maximum exists is approximately $s/D \approx 16$.

B. Comparison to experimental data

Burattini *et al* [14] created a jet by passing air through a round orifice into a large laboratory room with no cross-flow ($\mathbf{u}_a = 0$). The experiment was set up in such a way that there was no buoyancy difference between the jet and the ambient environment. This ensures that the vol-

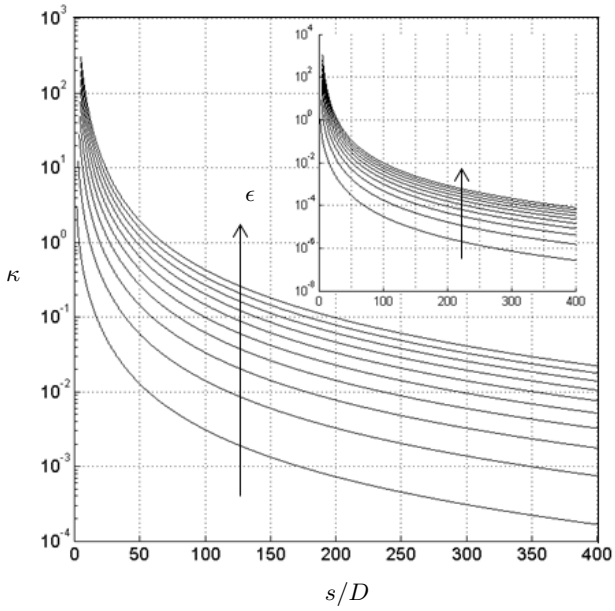

FIG. 4: Evolution of κ and ϵ (inset) with a varying effluent exit velocity, which was varied from 5m/s to 50m/s in steps of 5m/s. The arrows indicate the direction of increasing exit velocity. Other relevant model parameters and initial values are the same as those in Figure 2.

umetric expansion coefficient (β) is constant. Velocity measurements were taken using a hot wire anemometer and a single set of initial conditions was used for all of the data. The diameter of the orifice was 55mm, the efflux velocity was 35.1m/s and the viscosity of the air was $1.5 \times 10^{-5}\text{m}^2/\text{s}$. The effect of varying initial conditions on experimental outcomes can be found in Reference [15]. Figure 7 shows the measured values of κ, and ϵ from [14] as well as the result of the model solution for these quantities. The difference between the model results and experimental measurements for κ and ϵ was on average 0.69% and 1.56% with standard deviations of 3.08% and 6.37%, respectively. For both parameters the error never went over 9.8%.

The absence of a transport equation for ϵ in Reference [12] left the system incomplete without an empirical relationship for ϵ. An example of such a relationship is

$$\epsilon = c_\kappa \frac{\kappa^{3/2}}{L_\kappa} \tag{20}$$

where L_k is the integral length scale for κ [12]. As ϵ is known from the solution of its transport equation, Eq. 20 it can be leveraged to yield c_κ or L_κ. Integral length scales for u, and v are determined from similar equations to that in Eq. 20, $L_i = c_i \kappa^{3/2}/\epsilon$. The empirical constants c_i are chosen to best fit the data. The data taken from Ref. [14] and the result from the model solutions are shown in Figure 8.

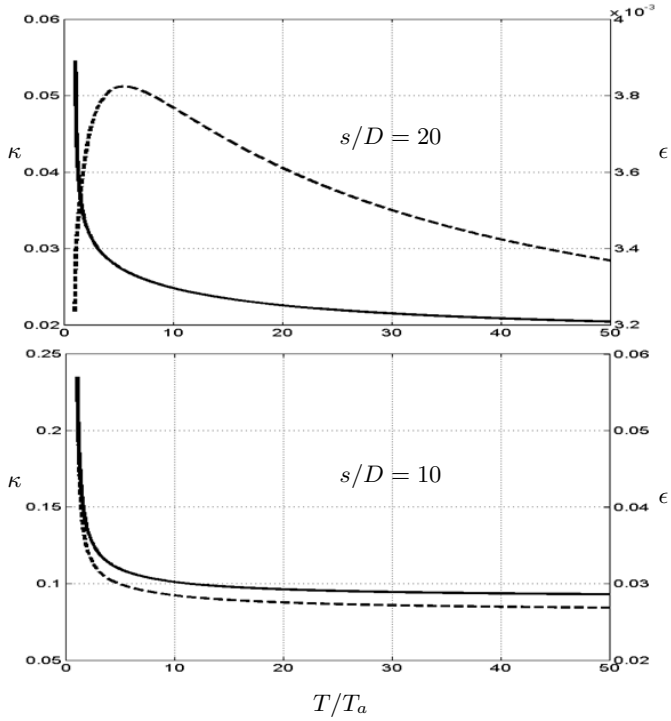

FIG. 5: Values of κ (solid) and ϵ (dashed) with a varying excess effluent temperature (T/T_a), at 10 (bottom) and 20 (top) stack diameters above the top of the stack. Other relevant model parameters and initial values are the same as those in Figure 2.

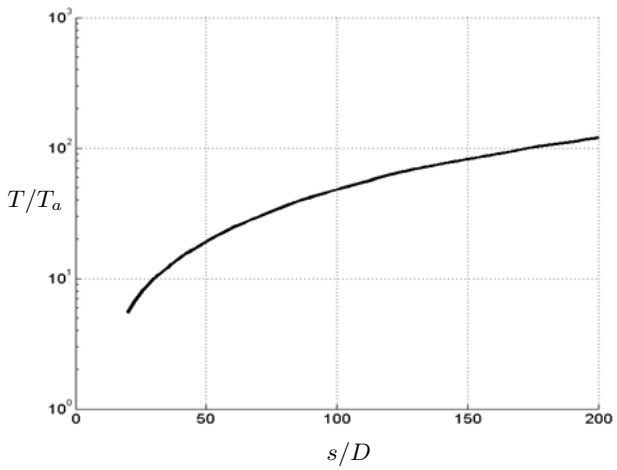

FIG. 6: Excess initial temperature (scaled by the ambient) of local maximum value of ϵ as a function of altitude above the exit point of the stack. Relevant model parameters and initial values are the same as those in Figure 2.

IV. CONCLUSIONS

This study investigated the evolution of turbulent kinetic energy and eddy dissipation rate of a round turbu-

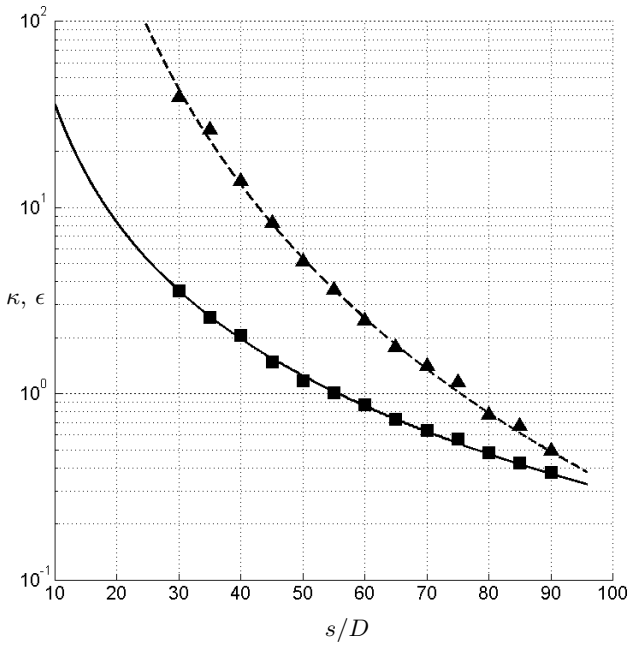

FIG. 7: A comparison of $\kappa - \epsilon$ model and the measured data from Reference [14]. The solid line and square symbols are the modeled and measured κ, respectively. The dashed line and triangle symbols are the modeled and measured ϵ, respectively. Relevant model parameters were $\sigma_\kappa^{1/2} = 1.343$, $\sigma_\epsilon^{1/2} = 1.505$, and $\sigma_T^{1/2} = 1.20$

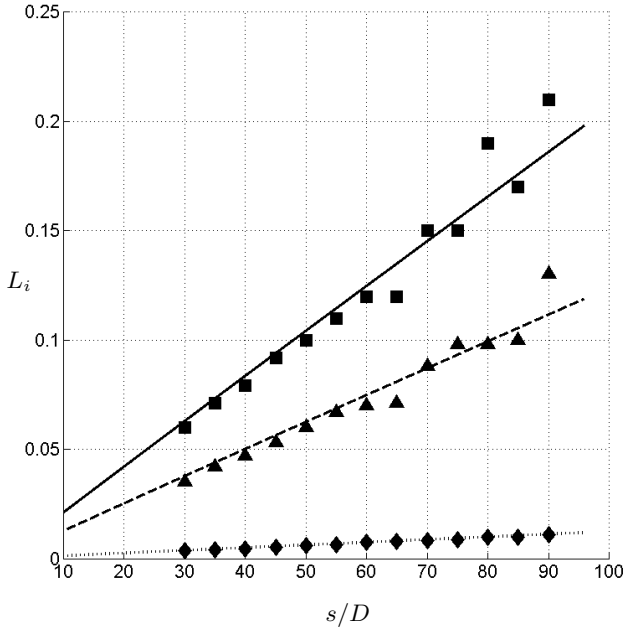

FIG. 8: A comparison of integral length scales L_u, L_v, and L_κ from the $\kappa - \epsilon$ model and the measured data from Reference [14]. The solid line and square symbols are the modeled and measured L_u, respectively. The dashed line and triangle symbols are the modeled and measured L_v, respectively. The dotted line and diamond symbols are the modeled and measured L_κ, respectively. Relevant model parameters are the same as those in Figure 7. The constants are $c_u = 0.40$, $c_v = 0.24$, and $c_\kappa = 0.024$.

lent buoyant jet, commonly formed above exhaust stacks at power plants or manufacturing facilities. Large enough Reynolds and Grashof numbers were assumed such that the flow can be treated as being entirely turbulent. A boundary layer approximation was made, and it was assumed that turbulent transport dominates molecular transport. Lastly, the system was reduced from partial to ordinary differential equations by assuming the form of the relevant fields is Gaussian and integrating across a cross section to yield an integral flux model. The result was a set of two coupled differential equations which couple as well with a model for the mean characteristics of the flow adopted with modification from Reference [2].

Integration of the system of equations yields results for the mean flow consistent with previous works [2]. The response of the system to changes in initial conditions (effluent temperature and velocity), as well as physical conditions (stack diameter) were investigated for illustrative purposes. Scenarios were devised to compare with experimental measurements of turbulent quantities. The results of Burattini *et al* [14] experiments for turbulent fluctuations in the velocity field and derived integral length scales compared favorably against the predicted output of the derived model.

While employing empirical calculations to compute the turbulent quantities from the mean flow can give insight into the dynamics of the turbulent motion, use of the evolution equations by employing an integral flux model reduces their complexity to the point where the problem is very tractable to most numerical ODE routines.

Acknowledgments

The authors acknowledge thoughtful feedback from S. Adam Blake, and Michael J. Mills.

Notice

This work was produced for the U.S. Government under Contract DTFAWA-10-C-00080 and is subject to Federal Aviation Administration Acquisition Management System Clause 3.5-13, Rights In Data-General, Alt. III and Alt. IV (Oct. 1996).

The contents of this document reflect the views of the author and The MITRE Corporation and do not necessarily reflect the views of the FAA or the DOT. Neither the Federal Aviation Administration nor the Department of Transportation makes any warranty or guarantee, expressed or implied, concerning the content or accuracy of these views. ©2012 The MITRE Corporation. As such, the Government retains a nonexclusive, royalty-free right

to publish or reproduce this document, or to allow others to do so, for Government Purposes Only.

Approved for public release; distribution unlimited. 12-4989.

APPENDIX A: ALGEBRAIC EXPRESSIONS

The following three algebraic expressions for $\overline{u_i u_j}$, $\overline{u_i T'}$, and $\overline{T'^2}$ are given here for completeness. Derivation of these expressions begins with general transport equations for these quantities. This study focuses on vertical buoyant jets which represent a vertical shear layer. As an approximation of these flows, convective and diffusive transport of turbulent flux and stress can be neglected due to slowly evolving nature of the flow. Complete details of this derivation can be found in [11]. The expressions are

$$\overline{u_i u_j} = \kappa \left[\frac{2}{3}\delta_{ij} \frac{c_1 + c_2 - 1}{c_1} - \frac{1 - c_2}{\epsilon c_1} \left(\overline{u_i u_l} \frac{\partial U_i}{\partial x_l} + \overline{u_j u_l} \frac{\partial U_i}{\partial x_l} + \beta g_i \overline{u_j T'} + + \beta g_j \overline{u_i T'} \right) \right], \tag{A1}$$

$$\overline{u_j T'} = \frac{1}{c_{1T}} \frac{\kappa}{\epsilon} \left[\overline{u_i u_l} \frac{\partial T}{\partial x_l} - (1 - c_{2T}) \overline{u_l T'} \frac{\partial U_i}{\partial x_l} - (1 - c_{3T}) \beta g \overline{T'^2} \right], \tag{A2}$$

and

$$\overline{T'^2} = -2R \frac{\kappa}{\epsilon} \overline{u_l T'} \frac{\partial T}{\partial x_l}. \tag{A3}$$

APPENDIX B: AUXILIARY QUANTITIES

There are several quantities in Eqs. 13 and 14 which arise from integration and manipulation of the governing equations and are given in this section. The expressions for K_i are

$$K_1 = 2 \frac{\sigma_\kappa^2}{(2 - (\sigma_\kappa/\sigma_\epsilon) + 2\sigma_\kappa)^2} \tag{B1}$$

$$K_2 = 2h_2 \frac{(\sigma_\kappa^2/\sigma_T)}{(3 - 2(\sigma_\kappa/\sigma_\epsilon) + (\sigma_\kappa/\sigma_T) + \sigma_\kappa)^2} \tag{B2}$$

$$K_3 = 2h_3 \frac{(\sigma_\kappa/\sigma_T)^2}{(4 - 3(\sigma_\kappa/\sigma_\epsilon) + 2(\sigma_\kappa/\sigma_T))^2} \tag{B3}$$

$$K_4 = \frac{1}{2}\sigma_\epsilon \tag{B4}$$

and M_i are

$$M_1 = 2 \frac{\sigma_k^2}{(1 + 2\sigma_k)^2} \tag{B5}$$

$$M_2 = 2h_2 \frac{(\sigma_\kappa^2/\sigma_T)}{(2 + (\sigma_\kappa/\sigma_T) - (\sigma_\kappa/\sigma_\epsilon) + \sigma_\kappa)^2} \tag{B6}$$

$$M_3 = 2h_3 \frac{(\sigma_\kappa/\sigma_T)^2}{3 + 2(\sigma_\kappa/\sigma_T) - 2(\sigma_\kappa/\sigma_\epsilon)^2} \tag{B7}$$

$$M_4 = \frac{\sigma_\kappa}{2\left[2(\sigma_\kappa/\sigma_\epsilon) - 1\right]} \tag{B8}$$

The values of h_i are

$$h_2 = C_\mu \frac{1}{c_{1T}} \left[1 + \frac{1}{c_{1T}} (1 - W) \frac{1}{W} \right], \tag{B9}$$

$$h_3 = \frac{4}{3} \frac{1}{c_{1T}^2} R (1 - c_{3T})(1 - W) \tag{B10}$$

where R is the gas constant, $W = (1 - c_2)/c_1$, $C_\mu = 2W(1 - W)/3$, and the empirical constants c_{iT}, $C_{i\epsilon}$ and c_i are given in Reference [11]. However, as a result of applying Eq. 12 to Eqs 6 and 7, several of the experimentally determined parameters no longer remain in the governing equations (13) and (14).

[1] P Best, L Jackson, C Killip, M Kanowski, and K. Spillane. Aviation safety and buoyant plumes. In *Clean Air*, 2003.

[2] G. H. Jirka. Integral model for turbulent buoyant jets in unbounded stratifed flows. part i: Single round jet. *Environmental Fluid Mech.*, 4:1–56, 2004.

[3] B. R. Morton, Taylor G. I., and Turner J. S. Turbulent gravitational convection from maintained and instantaneous sources. *Proc. Roy. Soc. London A*, 234:1–23, 1956.

[4] H. Reichardt. Uber eine neue theorie der freien turbulenzen. *ZAMM*, 21:257–264, 1941.

[5] B. R. Morton. Forced plumes. *J. Fluid Mech.*, 5:151–163, 1959.

[6] J. S. Turner. Turbulent entrainment: The development of the entrainment assumption, and its application to geophysical flows. *J. Fluid Mech.*, 173:431–471, 1986.

[7] J. W. Glendening, J. A. Businger, and R. J. Farber. Improving plume rise prediction accuracy for stable atmospheres with complex vertical structure. *JAPCA*, 134:1128–1133, 1984.

[8] P. N. Papanicolaou and E. J. List. Investigations of round vertical turbulent buoyant jets. *J. Fluid Mech.*, 195:341–391, 1988.

[9] H. Wang. Second-order integral model for a round turbulent buoyant jet. *J. Fluid Mech.*, 459:397–428, 2002.

[10] I. R. Wood, R. G. Bell, and D. L. Wilkinson. *Ocean Disposal of Wastewater*. World Scientific Publishing Company Incorporated, 1993.

[11] M. S. Hossain and W. Rodi. A turbulence model for buoyant flows and its application to vertical buoyant jets.

In *Turbulent buoyant jets and plumes 6*, pages 121–178. Pergamon, 1982.

[12] W. Rodi. *Turbulence Models and Thier Application in Hydraulics – A State of the Art Review.* Book Publication of International Association for Hydraulic Research, Delft, Neatherlands, 1990.

[13] J. O. Hinze. *Turbulence 2nd Ed.* McGraw Hill Co., New York, 1975.

[14] P. Burattini, R. A. Antiona, and L. Danaila. Similarity in the far field of a turbulent round jet. *Phys. Fluids*, 17(025101), 2005.

[15] P. Burattini, R. A. Antiona, S. Rajagopalan, and M. Stephens. Effects of initial conditions on the near-field development of a round jet. *Exp. Fluids*, 37(56), 2004.